

Reflectionless anisotropic multilayers for both polarisations at grazing incidence

Dean A. Patient*  and Simon A.R. Horsley

School of Physics and Astronomy, University of Exeter, EX4 4QL Exeter, UK

Received: 17 November 2021 / Accepted: 8 April 2022

Abstract. We find a method for designing anisotropic multilayer profiles that are reflectionless at grazing incidence, for both electromagnetic polarisations. The Helmholtz equation for grazing incidence propagation through an anisotropic multilayer can be factorised into a pair of equations of the form $\hat{a}^\dagger \hat{a} \varphi = 0$. Solutions of $\hat{a} \varphi = 0$ then determine two of the three principal values of the permittivity. Imposing the additional constraint of uniaxial anisotropy, we find a pair of coupled equations for the profile of both permittivity components such that neither polarisation is reflected.

1 Introduction

As the angle of incidence approaches 90 degrees, electromagnetic (EM) waves are nearly always completely reflected from an interface. Although this can be useful for increasing the signal from a weakly scattering object, grazing incidence is problematic for e.g. radar absorbers [1], and the perfectly matched layers used in simulations [2]. The simplest example of complete reflection at grazing can be found in the Fresnel equations where, in the limit of grazing incidence, $|r_{TE/TM}|^2 \rightarrow 1$.

There are exceptions however: free standing graphene layers have been observed not to reflect TM polarised waves at grazing incidence, although the addition of dielectric substrates above and below the graphene negates this effect [3]. The Pöschl-Teller potential is perhaps the most famous non-trivial dielectric profile that will not reflect waves incident at any angle, for a particular frequency [4]. Another example is given through transformation optics, where anisotropic magnetodielectric media [5,6] do not reflect waves at any angle. In this work, we focus our attention to the limit of grazing incidence, and look for structures that do not reflect in this limit.

There is an analogy between the reflection of electromagnetic waves at grazing incidence and quantum mechanics, the cosine squared of the angle of incidence being equivalent to the energy of a quantum particle. Approaching zero-energy, a quantum particle incident onto a potential well is also typically completely reflected, and exceptions to this rule are known as ‘threshold anomalies’. These arise when the potential well supports a

so-called half-bound state (HBS) [7], allowing the particle to transmit with certainty [8]. Isotropic permittivity profiles can support analogues of these states [9]. In previous work we designed such media using the factorisation method [10] to decompose the Helmholtz equation into ‘raising’ and ‘lowering’ operators. Enforcing that the ‘lowering’ operator has a zero-eigenvalue leads to an isotropic permittivity profile that do not reflect transverse electric (TE) waves at grazing incidence. Although the design of reflectionless layered dielectrics is well established [11], the approach given here is new and uses an equivalent continuous description of the dielectric profile to derive structures supporting HBSs, corresponding to zero reflection of EM waves close to grazing incidence.

Using isotropic non-magnetic materials prevented our previous theory from being applicable to design materials that are reflectionless for both polarisations. Here we extend that theory, considering anisotropic non-magnetic materials where the permittivity is a rank 2 tensor [12]. Although anisotropic materials can be extremely subtle when none of the principal axes are parallel to the surface normal (see for instance the recent discovery of ‘Brewster absorbers’ [13]), we leave this general case for future work. We find that for anisotropic media both the TE and transverse magnetic (TM) Helmholtz equations can be factorised into ‘raising’ and ‘lowering’ operators, and we can find materials such that the ‘lowering’ operators have a simultaneous eigenstate with eigenvalue zero. Enforcing the condition that the permittivity tensor is uniaxial, with the optical axis along the surface normal we are then able to design materials where both polarisations do not reflect at grazing incidence, irrespective of the plane of incidence.

* e-mail: dp348@exeter.ac.uk

2 Maxwell's equations in an anisotropic multilayer

Consider an anisotropic multilayer with permittivity $\bar{\epsilon}$, extending from $x = -L/2$ to $x = L/2$, with an isotropic cladding layer with permittivity ϵ_b outside. We assume the system is translationally invariant in the y - z plane, and neglect magnetic properties ($\mu = 1$). The principal axes of the multilayer align with the x , y , and z axes, and for the time being we do not assume any relation between the principal values. With these assumptions the tensor $\bar{\epsilon}$ takes the form

$$\bar{\epsilon}(x) = \begin{pmatrix} \epsilon_x(x) & 0 & 0 \\ 0 & \epsilon_y(x) & 0 \\ 0 & 0 & \epsilon_z(x) \end{pmatrix}. \quad (1)$$

For a fixed wavenumber $k_0 = \omega/c$, Maxwell's equations reduce to

$$\begin{aligned} \nabla \times \mathbf{E} &= ik_0 \eta_0 \mathbf{H} \\ \nabla \times \eta_0 \mathbf{H} &= -ik_0 \bar{\epsilon}(x) \cdot \mathbf{E} \end{aligned} \quad (2)$$

where $\eta_0 = \sqrt{\mu_0/\epsilon_0}$ is the impedance of free space. Combining the two Maxwell equations (Eq. (2)) we can eliminate either the electric or magnetic field, which leads to the pair of vector Helmholtz equations

$$\nabla \times \nabla \times \mathbf{E} - k_0^2 \bar{\epsilon} \cdot \mathbf{E} = 0, \quad (3)$$

and

$$\nabla \times \bar{\epsilon}^{-1} \cdot \nabla \times \mathbf{H} - k_0^2 \mathbf{H} = 0. \quad (4)$$

We assume propagation in the x - y plane, where the y component of the wave-vector is fixed as k_y . The EM field can then be written as a sum of two polarisations; TE $\mathbf{E} = \varphi(x) e^{ik_y y} \mathbf{z}$; and TM $\mathbf{H} = \psi(x) e^{ik_y y} \mathbf{z}$. Substituting these forms of the electric and magnetic fields into equations (3) and (4) then gives us the second order ordinary differential equations

$$\left(\frac{d^2}{dx^2} + k_0^2 \epsilon_z(x) - k_y^2 \right) \varphi(x) = 0, \quad (TE) \quad (5)$$

and

$$\left(\frac{d}{dx} \frac{1}{\epsilon_y(x)} \frac{d}{dx} + k_0^2 - \frac{k_y^2}{\epsilon_x(x)} \right) \psi(x) = 0. \quad (TM) \quad (6)$$

While the TE polarisation is sensitive to only the principal value of the permittivity along the z -axis, the TM polarisation depends on both the x and y principal values. Unless the material is uniaxial ($\epsilon_y = \epsilon_z$), the response to incident radiation depends on the plane of

incidence. In Section 4 we consider the restriction to uniaxial media.

3 Factorisation at grazing incidence

In previous work [9] we gave a method for designing materials where there is zero reflection for one polarisation at grazing incidence ($k_y \rightarrow \sqrt{\epsilon_b} k_0$). One way to characterise whether a material is reflectionless is to find whether the two solutions to the Helmholtz equation outside the material can be written as sine and cosine standing waves (e.g. the solutions are *either* $\varphi = \sin(kx)$, or $\varphi = \cos(kx)$ everywhere $\epsilon = 1$). If the solutions take this form then waves $\varphi = \cos(kx) \pm i \sin(kx) = \exp(\pm ikx)$ can be constructed that are purely right or left going on both sides of the material. In the limit of grazing incidence ($k \rightarrow 0$), the sine and cosine functions become $\sim x$ and ~ 1 outside the material. To ensure that our multilayer is reflectionless at grazing incidence we impose the condition that our solution tends to a constant outside the dielectric (is proportional to ~ 1). This implies the second solution is proportional to x outside, and we can construct the limiting case of travelling waves $\exp(\pm ikx) \sim 1 \pm ikx$ on the incidence and transmission sides of the material, implying that it is reflectionless. Such solutions that tend to a constant at infinity are known as HBSs. The field is 'bound' to the material, but is non-normalisable. We previously found isotropic dielectric profiles $\epsilon(x)$ supporting HBSs for only TE polarised waves at grazing incidence, and verified that these led to zero reflection. We now look for *anisotropic* multilayers that don't reflect grazing incidence waves of either polarisation. To control the solutions to the Helmholtz equations (5) and (6), we use the formalism adopted in supersymmetric quantum mechanics, factorising both equations into a product of 'creation' and 'annihilation' operators, $\hat{a}^\dagger \hat{a} \varphi = 0$, and $\hat{b}^\dagger \hat{b} \psi = 0$. The Helmholtz equation for TE waves, equation (5), can then be written as

$$\hat{a}^\dagger \hat{a} \varphi = \left(-\frac{d}{dx} + k_0 \beta(x) \right) \left(\frac{d}{dx} + k_0 \beta(x) \right) \varphi(x) = 0, \quad (7)$$

and the TM case, equation (6) as

$$\begin{aligned} \hat{b}^\dagger \hat{b} \psi &= \left(-\frac{1}{\epsilon_y(x)} \frac{d}{dx} + k_0 \alpha(x) \right) \left(\frac{1}{\epsilon_y(x)} \frac{d}{dx} + k_0 \alpha \right) \psi(x) \\ &= 0, \end{aligned} \quad (8)$$

where the functions $\alpha(x)$ and $\beta(x)$ are zero outside of the slab and determine the permittivity. Comparing the factorised Helmholtz equations (7) and (8) (for $k_y = \sqrt{\epsilon_b} k_0$) to the original expressions, equations (5) and (6), we find the permittivity components $\epsilon_z(x)$ and $\epsilon_x(x)$ in terms of the arbitrary functions $\alpha(x)$ and $\beta(x)$,

$$\epsilon_z(x) = \epsilon_b + \frac{1}{k_0} \frac{d\beta(x)}{dx} - \beta(x)^2, \quad (9)$$

and

$$\varepsilon_x(x) = \left(\varepsilon_b - \frac{1}{k_0} \frac{d\alpha(x)}{dx} + \varepsilon_y(x)\alpha(x)^2 \right)^{-1} \quad (10)$$

both of which tend to unity when $|x| > L/2$. From this point forward we assume that the cladding layer is free space, $\varepsilon_b = 1$.

One solution to each of the factorised equations (5) and (6) can be written down immediately, being that which is annihilated by the \hat{a} operator. In the case of TE waves, this is the solution to $(\partial_x + k_0\beta)\varphi = 0$, which can be integrated to give

$$\varphi_1(x) = \varphi_1(-L/2)\exp\left[-k_0\int_{-L/2}^x\beta(x')dx'\right], \quad (11)$$

Similarly for TM radiation, integration of $b\psi = 0$ gives

$$\psi_1(x) = \psi_1(-L/2)\exp\left[-k_0\int_{-L/2}^x\varepsilon_y(x')\alpha(x')dx'\right], \quad (12)$$

where $k_0 = 1$, $L = \lambda$ throughout. L can be chosen arbitrarily, with smaller values (relative to the wavelength) increasing the values of the derivatives in equations (9) and (10). To satisfy the condition $\psi, \varphi \sim 1$ required for a HBS, the integrals with the exponents of equations (11) and (12) must equal zero when taken over the entire multilayer. We impose this through choosing both $\alpha(x)$ and $\varepsilon_y(x)\beta(x)$ as odd functions of x . In this case the field is equal on the two sides of the slab e.g. $\varphi_1(-L/2) = \varphi_1(L/2)$. As $\alpha(x)$ and $\beta(x)$ are zero outside of the slab the fields φ and ψ are HBSs, equalling the same constant everywhere in this region. We note that in its current form, this framework can only be applied to grazing incidence waves. Taking advantage of the fact that in the limit of grazing incidence, the solutions to the Helmholtz equations outside the material are not propagating waves, as well as knowing the solution has to take the form of a HBS, we demonstrate a way to design real-valued dielectric materials that will not reflect grazing incidence waves. If one wanted to instead consider angles off-grazing, equations (11) and (12) would have to be modified into complex functions by changing $k_0\beta \rightarrow ik_0\beta$, $k_0\alpha \rightarrow ik_0\alpha$. This ensures that the solutions to the fields φ_1, ψ_1 are propagating solutions, and then the permittivity components satisfy the complex valued functions

$$\varepsilon_z(x) = \sin^2\theta + \frac{i}{k_0} \frac{d\beta(x)}{dx} + \beta(x)^2, \quad (13)$$

and similarly for equation (10), for an angle of incidence θ . These non-Hermitian permittivity profiles (i.e. containing a distribution of gain and loss) have been derived before, in a different context, both using topology [14], and in disordered media exhibiting ‘constant-intensity waves’ [15].

As an initial example, we assume that inside the slab the y principal value of the permittivity $\varepsilon_y(x) = \text{const}$. This simplifies the formalism for TM waves, as the permittivity ε_x depends on $\alpha(x)$ alone. To construct the spatially dependant ε_x and ε_z profiles, the two functions $\alpha(x), \beta(x)$

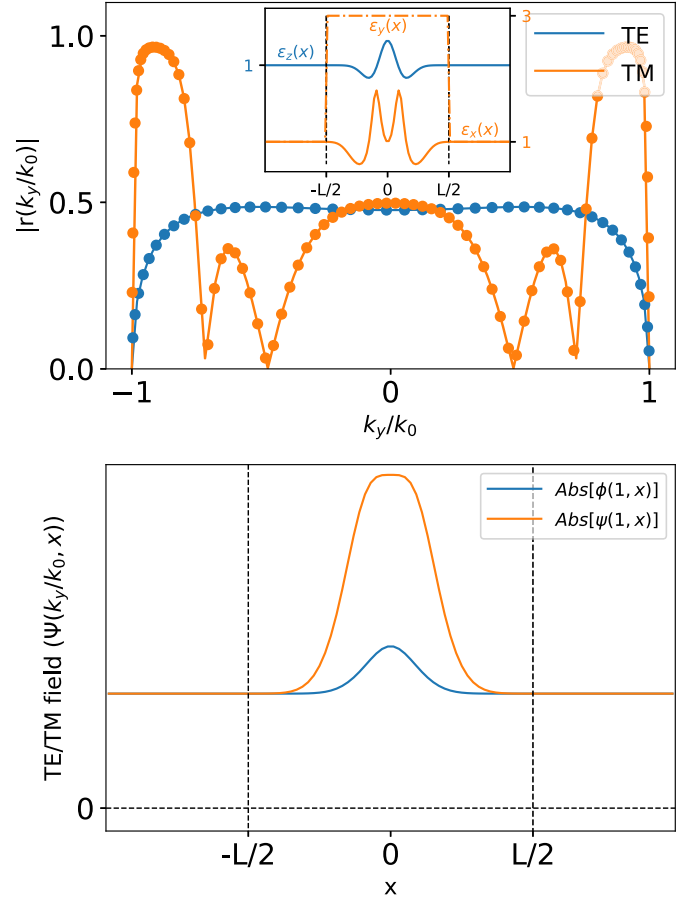


Fig. 1. An anisotropic material with a constant $\varepsilon_y(x)$ and tailored $\varepsilon_x(x), \varepsilon_z(x)$ (inset) ($\beta(x) = \cos(\pi x/L)^2 \sin(2\pi x/L) \exp(-x^2)$, $\alpha(x) = x^2 \sin(2\pi x/L) \exp(-x^2)$) inside the slab is designed such that it (top) does not reflect either TE or TM waves at grazing incidence. The results obtained from COMSOL Multiphysics are shown as dots. The field profiles at grazing incidence (bottom) are shown to decay to non-zero constants of equal amplitudes outside the slab region, as required for a half-bound state.

are chosen as arbitrary odd functions that decay to zero smoothly at the boundary of the material. Using the ‘odeint’ integrator in the SciPy library [16], we solve the Helmholtz equation numerically to calculate the fields, and from that the reflection coefficients. The results show that the choices for the permittivity functions allow the material to support a HBS for TE and TM waves, which allow for zero reflection at grazing, as is shown in Figure 1. However we note that in the absence of the condition that the material is uniaxial ($\varepsilon_y = \varepsilon_z$), this result only holds for incidence in the x - y plane. Also shown in Figure 2 are the absolute values of the field distributions for TE and TM incidence for both normal and grazing angles, computed using COMSOL Multiphysics [17]. For these simulations, we used a port that emitted either a TE or TM wave $\mathbf{E}/\mathbf{H} = (0, 0, E/H)$ to produce reflectivity simulations for the two cases. Equations (9) and (10) were used directly with the equations for $\beta(x)$ and $\alpha(x)$ given in Figure 1 as functions to create the anisotropic material in the model

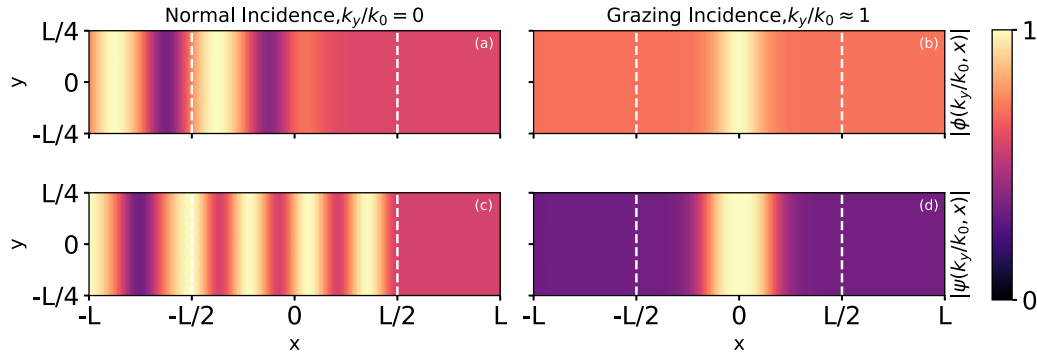


Fig. 2. The field distributions (for the device in Fig. 1), $|\phi|$ of a TE wave incident at normal (a) and grazing ($\theta = 89^\circ$) (b). Similarly for the TM case, $|\psi|$ for normal (c) and grazing ($\theta = 89^\circ$) (d). At normal incidence, the absolute value of the field is not constant on the left, indicating there is reflection, whereas for grazing, the equal field amplitude on the two sides of the profile shows that there is no reflection.

($\bar{\epsilon} = \mathbf{I}(\epsilon_x(x), 3, \epsilon_z(x))$, where \mathbf{I} is the 3×3 identity matrix) with free space outside to visualise the HBSs. As can be seen, at normal incidence for both cases, there is a ‘beating’ effect, showing that there is interference between the incident and reflected waves. At grazing incidence, we see that the field has the same amplitude on the left and right hand side of the material – this is evidence that there is complete transmission. Further, we consider the case where one of the permittivity components, $\epsilon_y(x)$ is negative. This constraint that the y -component is metal-like, enforces that our material is now hyperbolic [18]. For our devices, we make the y -component of the permittivity take a negative value. The results are given in Figure 3. The choice of a negative valued component of the permittivity means that although the TE case is unchanged, for TM waves the material now acts like a graded metal. This reflects all incidence TM waves over the complete angular range, except in a narrow window very close to grazing incidence.

4 Uniaxial multilayers

We now impose the condition that the permittivity tensor is uniaxial with the optical axis being oriented along x ($\epsilon_y = \epsilon_z$) [19]. With this assumption, the multilayer is invariant to rotations around the x -axis, and therefore our results do not depend on the assumption of incidence being in the x - y plane. We thus derive multilayers that are reflectionless at grazing incidence for *both* polarisations. As stated above, the vanishing of the exponent in equation (12) requires the function $\epsilon_y(x)\alpha(x)$ to be odd in x . Taking $\beta(x)$ as an odd function of x we can see from equation (9) that ϵ_z is an even function. Assuming $\epsilon_y(x) = \epsilon_z(x)$ in equation (10) we see that ϵ_y is similarly an even function if $\alpha(x)$ is odd. This shows consistency with the assumption that $\epsilon_y(x)\alpha(x)$ is odd, so that grazing incidence reflectionless uniaxial media can be found from the coupled equations formed by replacing $\epsilon_y(x)$ with $\epsilon_z(x)$ in equations (9) and (10). These are solved in two steps, through first picking an odd function $\beta(x)$ to find $\epsilon_y(x) = \epsilon_z(x)$. After this we choose another odd function $\alpha(x)$ from which—along with $\epsilon_z(x)$ —we can find $\epsilon_x(x)$. An example result of

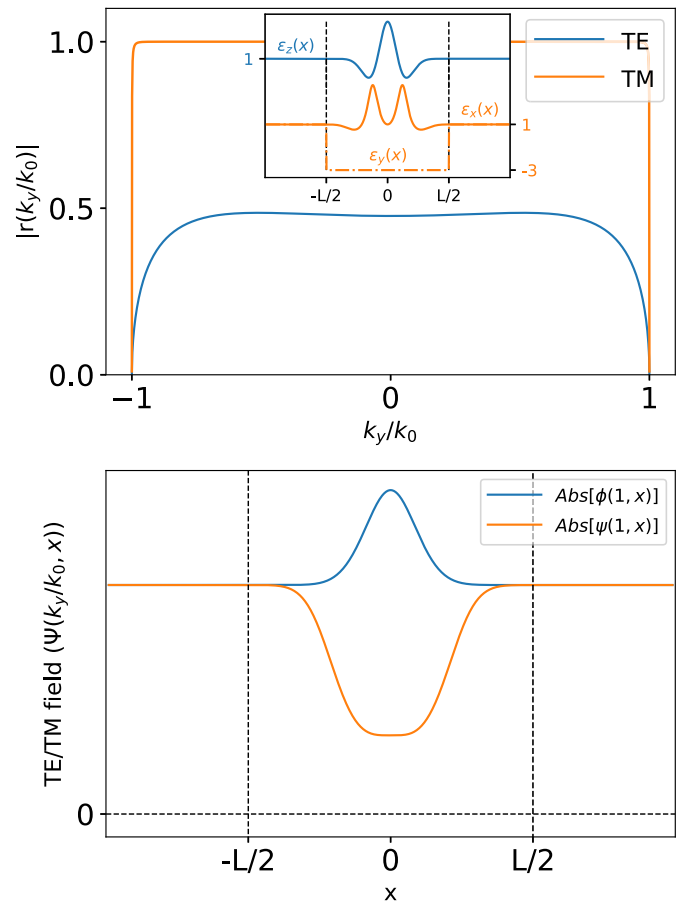


Fig. 3. A hyperbolic material with constant $\epsilon_y = -3$, and ϵ_x, ϵ_z staying the same as in Figure 1. The top panel shows that although the TM case has almost complete reflection, at grazing incidence the profile of $\epsilon_x(x)$ ensures there is no reflection at grazing.

this method is given in Figure 4, showing designs for uniaxial media where HBSs are supported for both polarisations at grazing incidence.

We find that in the uniaxial design (Fig. 4) the transition to zero reflection at grazing is smoother than in the case of ‘standard’ anisotropy (Fig. 1), where the reflection close to

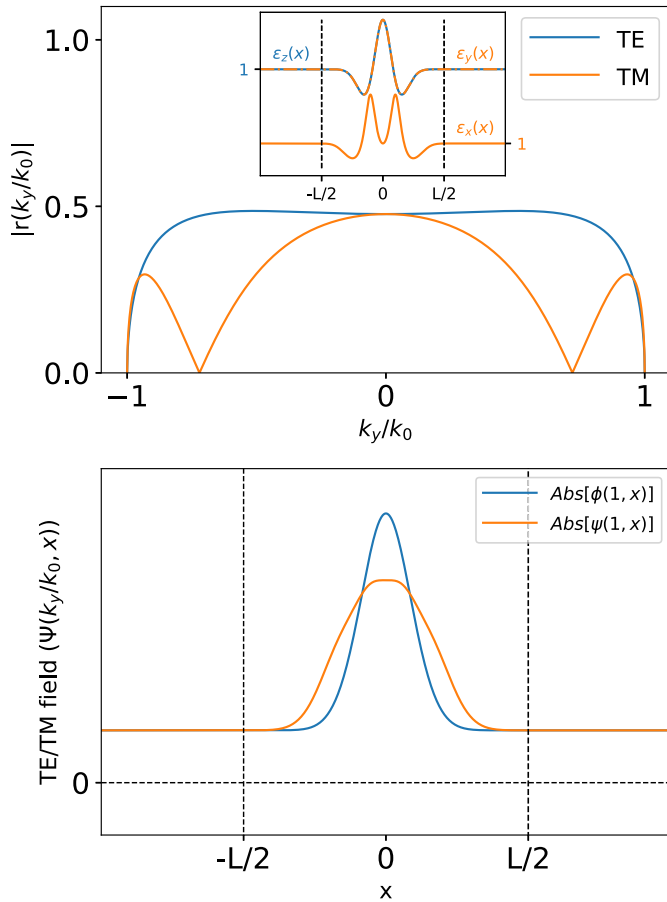


Figure 4. A uniaxial anisotropic material is defined as one whose $\varepsilon_y(x) = \varepsilon_z(x) \neq \varepsilon_x(x)$. The two permittivities $\varepsilon_z(x)$, $\varepsilon_x(x)$ (inset) ($\beta(x)$ and $\alpha(x)$) are the same as in Fig. 1) are designed to ensure that the material exhibits zero reflection at grazing (top) as a result of the material supporting a HBS for both polarisations at grazing incidence (bottom).

grazing is near unity, before a sharp descent to zero reflection at grazing. The only disparity between these two cases is the choice of $\varepsilon_y(x)$, where in one case there is a large discontinuity at the material edges, and in the other, the profile tends to the background value smoothly. This discontinuity contributes to the sharp rise in reflectivity close to grazing, and in Figure 5 we show (TE) results for a profile $\beta_z(x)$ that has a discontinuous permittivity at the material boundary, finding a corresponding sharp rise in the reflection coefficient as a function of angle.

5 Summary and conclusions

Unlike the isotropic multilayers that were the focus of our previous study [9], for anisotropic multilayers the two Helmholtz equations for TE and TM polarisations can be simultaneously factorised into the form $\hat{a}^\dagger \hat{a} \phi = 0$; the same factorisation used in the formalism of supersymmetric quantum mechanics. This procedure builds on the novel method for designing non-reflecting optical materials that was explored in [9]: a new application of quantum

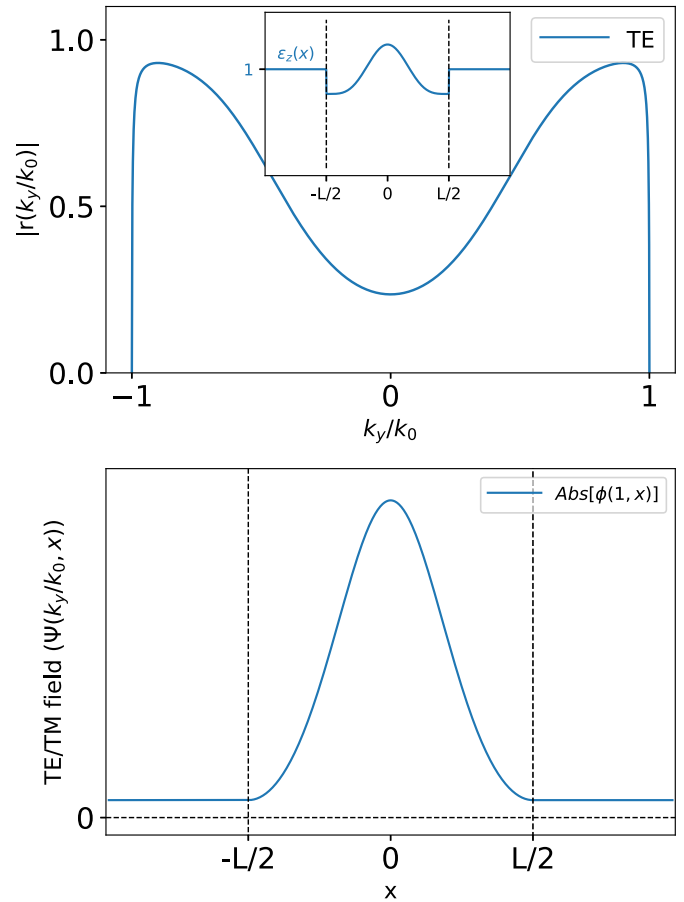


Fig. 5. A profile $\varepsilon_z(x)$ (inset) is designed to specifically have a large discontinuity at the boundary between the material and the vacuum. As a result, the reflectivity (top) exhibits large reflection at angles close to grazing but still goes to zero at grazing. The field profile (bottom) is given to show that the system still supports a HBS.

mechanical techniques to the design of optical materials. This can be done provided the principal values of the permittivity are of the form given in equations (9) and (10). Using this factorisation—demanding that $\hat{a} \phi = 0$ for both polarisations—we have given a method for designing anisotropic multilayers that do not reflect either polarisation at grazing incidence in a particular plane.

A feature in these materials is the necessity for the permittivity functions to take values less than the background value. Although for homogeneous media this would lead to total internal reflection (TIR), in these structures however, we have a rapidly varying, inhomogeneous material profile. Imposing the additional constraint that the vanishing reflection is independent of the plane of incidence we found that replacing $\varepsilon_y(x) \rightarrow \varepsilon_z(x)$ in equations (9) and (10), the resulting equations describe uniaxial media. We also investigated the angular bandwidth of the low reflection around grazing, finding that it can be modified through varying the contrast of one or mode of the permittivity values at the leading interface. The field profiles of the waves at grazing incidence show the material supports HBSs for both polarisations at any angle of incidence. In addition to numerical integration using

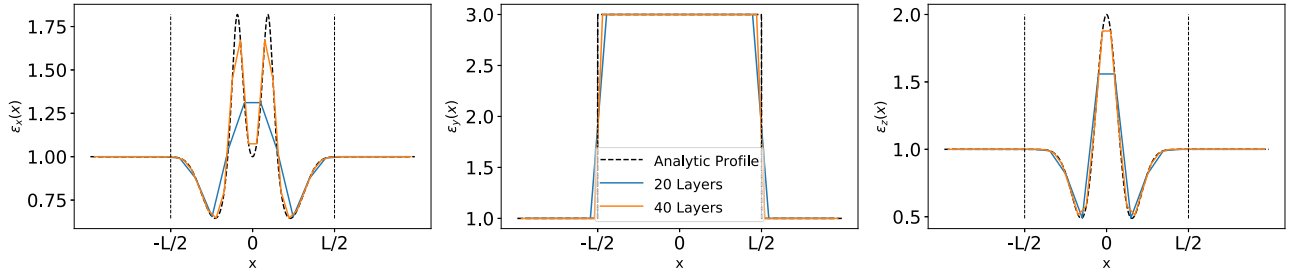


Fig. 6. The distribution for the x (left), y (middle) and z - (right) diagonal components of the permittivity tensor for the stacked structures of 20 and 40 layers compared to the analytic profiles (black dashed).

Python, we have further verified our findings using finite element simulations in COMSOL Multiphysics. Our results are both of fundamental interest, providing a new application of supersymmetric quantum mechanics, and may be of practical importance in the design of multilayers where large signals at grazing incidence are unwanted (e.g. in the design of absorbers).

The authors would like to acknowledge the Exeter Metamaterials CDT and the EPSRC (EP/L015331/1) for funding and supporting this research. SARH acknowledges financial support from a Royal Society TATA University Research Fellowship (RPG-2016-186).

Appendix: Stratified materials

We consider taking the continuous functions for the tensor $\bar{\epsilon}$ and splitting them up into a stratified material: N layers of homogeneous material. We no longer have to numerically solve the Helmholtz equations (Eqs. (5) and (6)), but rather we can apply the Transfer Matrix Method (TMM) [12] to analytically calculate the reflection coefficients, taking care to ensure that Maxwell's boundary conditions are satisfied across the interfaces of the anisotropic media. For a given angle of incidence k_y at a frequency k_0 from free space, the isotropic dispersion relation reads as

$$k_x^2 = \epsilon(x)k_0^2 - k_y^2, \quad (\text{A.1})$$

whereas in the case of anisotropic materials, we find that for a given layer, the dispersion relations read as

$$k_x^2 = \epsilon_z k_0^2 - k_y^2 \quad (\text{A.2})$$

for the TE case, and

$$k_x^2 = \epsilon_y k_0^2 - \frac{\epsilon_y}{\epsilon_z} k_y^2 \quad (\text{A.3})$$

for the TM case. Making these changes to the generic isotropic TMM code, allows our HBS structures to be modelled as layers of stacked dielectrics. Taking the permittivities from Figure 1 and converting the profiles into stacked layers (taking the average permittivity across some thickness $\delta = L/N$), we find that the permittivities

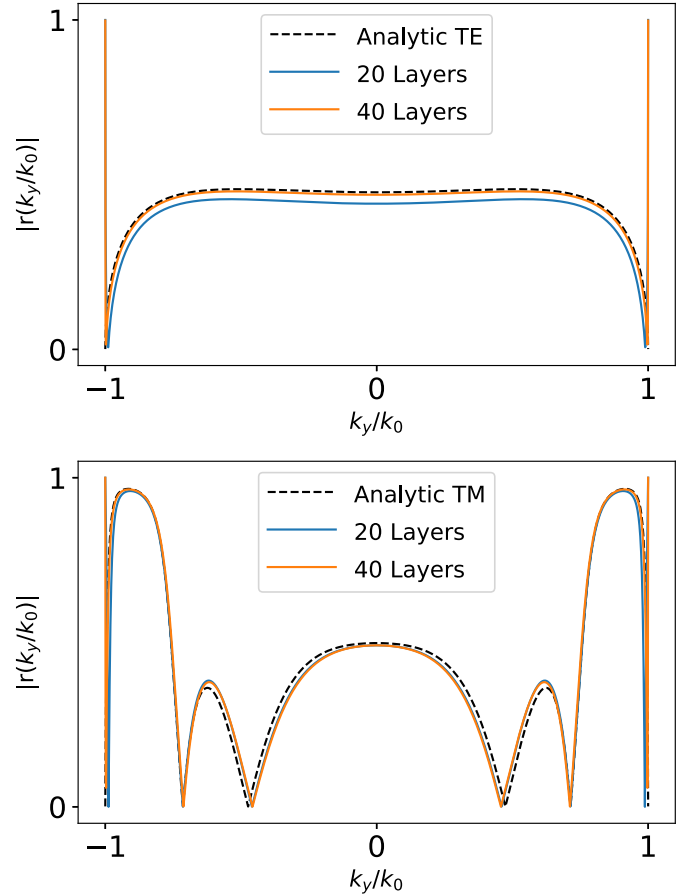


Fig. 7. The reflection coefficients for the TE (top) and TM (bottom) case are given for the multilayer approximations to the continuous profiles shown in Figure 1. The reflection coefficients are not affected significantly, there remaining a range of angles at almost grazing where the reflectivity is close to zero.

given in Figure 6 show that even a relatively small number (20) of layers is enough to accurately reconstruct the analytic reflection profiles, shown in Figure 7. The obvious consequence, however, of stratifying these materials is that even the small jumps in ϵ_n between layers will create unwanted reflection effects, and so the reflection at true grazing is no longer zero. However, the angular distribution of the reflection remains unchanged, and there is still low reflection close to grazing.

References

1. B.T. Dewitt, W.D. Burnside, IEEE Trans. Antennas Propag. **36**, 971 (1988)
2. W.C. Chew, J.M. Jin, Electromagnetics **14**, 325 (1996)
3. Y. Bludov, N.M.R. Peres, M.I. Vasilevskiy, J. Opt. **15**, 114004 (2013)
4. G. Pöschl, E. Teller, Zeit. Phys. **83**, 143 (1933)
5. J.B. Pendry, D. Schurig, D.R. Smith, Science **312**, 1780 (2006)
6. U. Leonhardt, T.G. Philbin, New J. Phys. **8**, 247 (2006)
7. P. Senn, Am. J. Phys. **56**, 916 (1988)
8. E.P. Wigner, Phys. Rev. **73**, 1002 (1948)
9. D.A. Patient, S.A.R. Horsley, J. Opt. **23**, 8 (2021)
10. F. Cooper, A. Khare, U.P. Sukhatme, Phys. Rep. **251**, 267 (1995)
11. R.E. Collin, Proc. IRE **44**, 539 (1956)
12. M. Born, E. Wolf, Principles of Optics (Elsevier, 2013)
13. J. Luo, H. Chu, R. Peng, M. Wang, J. Li, Y. Lai, Light Sci. Appl. **10**, 1 (2021)
14. S.A.R. Horsley, Phys. Rev. A **100**, 053819 (2019)
15. K.G. Makris, A. Brandstötter, P. Ambichl, Z.H. Musslimani, S. Rotter, Light Sci. Appl. 2017 **69** **6**, e17035 (2017)
16. P. Virtanen et al., Nat. Methods **17**, 261 (2020)
17. "COMSOL Multiphysics v. 6.0" (2022)
18. A. Poddubny, I. Iorsh, P. Belov, Y. Kivshar, Nat. Photonics **7**, 948 (2013)
19. J. Lekner, J. Phys.: Condens. Matter **3**, 6121 (1991)

Cite this article as: Dean A. Patient, Simon A.R. Horsley, Reflectionless anisotropic multilayers for both polarisations at grazing incidence, EPJ Appl. Metamat. **9**, 15 (2022)